

A Quasi-realistic Internet Graph

Paulo Salvador

DETI, University of Aveiro, Instituto de Telecomunicações, Aveiro, Portugal

Keywords: Internet, Graph Model, Quasi-realistic, Real IX and Submarine Cables.

Abstract: The existence of a realistic Internet interconnections model has been an important requirement to effectively support areas as routing optimization, routing security, and services QoS prediction. However, no usable and no useful models exist. The existing interconnection models are to (i) simplistic to be applicable in real scenarios, or (ii) incorporate too much uncorrelated information that cannot be used due to its complexity. This work presents the construction steps and final solution for a quasi-realistic graph that models the Internet as an all. The graph is based on all known Internet exchange points (IX) and landing points of all known submarine cables. The lack of information about interconnections between IX and landing points is extrapolated from simple rules that take into consideration Earth geographic characteristics. This approach results in a graph that includes all major corner stones of the Internet while maintaining a simple structure. This graph can then be used to predict connectivity and routing properties between any two geographical points in Earth. The proof-of-concept results, even with very simplistic assumptions as similar node and link loads and symmetric routing by the shortest path, show that the model allows the prediction of the round-trip time of traffic and number of nodes between any two Internet points with an acceptable average error.

1 INTRODUCTION

Internet complexity in terms of magnitude, unknown interconnectivity, and asymmetry restricts the construction of any useful and usable model. An Internet quasi-realistic model can be used in routing optimization studies, specially when properties of nodes, links and addressing can be totally controlled while maintaining a close to real structure of relations. Security topics, namely the ability to detect and locate sources of traffic redirection attacks (Pilosov and Kapela, 2008), can greatly benefit from a quasi-realistic Internet relations. Solutions based on constant motorization of round-trip time to a specific locations from multiple worldwide locations allow the detection of routing anomalies (Salvador and Nogueira, 2014). However, such mechanisms rely on an effective Internet model to identify and locate the source of illicit routing anomalies. Also, when deploying a worldwide scale service based on Content Distribution Networks (CDN) it is important to infer *a priori* the expected quality of service for users in diverse world locations and under multiple network conditions.

This paper addresses the construction of an Internet graph model based on real data, such as submarine cables landing points and IX locations, and con-

strained by Earth geographical characteristics. The resulting graph has an open structure where nodes and links have properties (e.g., IX name, landing point name, and geographic distances) and is open to define other properties (e.g., node load, link load, link speed, etc. . .).

The developed code for construction and final usable Internet graph are publicly available at graph.netconfs.net.

2 RELATED WORK

Several works on mapping of the Internet have been presented, however, they are restricted to cataloging and visualization of Internet nodes and connections. Durairajan *et al.* (Durairajan *et al.*, 2013; Durairajan *et al.*, 2015) constructed a geographic database of the Internet based on real data, which result is publicly available (internetatlas.org) and allows data visualization and analysis. However, such compilation of data is easily usable in studies because it requires data aggregations in a valid model that incorporates all interconnections and relation

3 INTERNET ELEMENTS AND INTERCONNECTIONS

3.1 Nodes

The Internet graph nodes will be all known IX and landing points from submarine cables from data publicly available compiled by TeleGeography. Submarine cable information is available on website TeleGeography Submarine Cable Map (www.submarinecablemap.com) and respective repository (github.com/telegeography/www.submarinecablemap.com). Internet exchanged information is available on website TeleGeography Internet Exchange Map (internetexchangemap.com) and respective repository (github.com/telegeography/www.internetexchangemap.com).

The available data in December 5th 2016, listed 1202 IX, however only 600 were considered. IX from the same provider at the same building or nearby buildings were merged and considered as a single IX node. At the same date, there were 368 listed submarine cables, with a total of 947 unique landing points (considering its identifier and geographical location). From the 947 unique landing points, two pairs of nodes had the same identifier but different however close geographic locations. Each of these pairs of points were merged into a single landing point. Therefore, only 945 landing points nodes were integrated into the graph.

3.2 Links

Internet link information is almost inexistent. The only real information must be extracted from the known submarine cables information, where is possible to assume that each cable landing point has a direct connection to all other landing points. However, the publicly available information does not define the order by which the landing points are connected, neither the geographic path that the cable follows. Therefore, all Internet oceanic links and respective path can be closely inferred from the available data by imposing constrains has geographic elevation (ocean depth) and geographic distances between points.

For Internet land links, available information is really limited by service providers and difficult to correlate with IX and landing points locations. Portals like Internet Atlas have information about some providers in restricted areas of the world, but is difficult to infer inter-connections between providers. In this work was choose a more heuristic approach in which land links were defined based on basic rules constrained

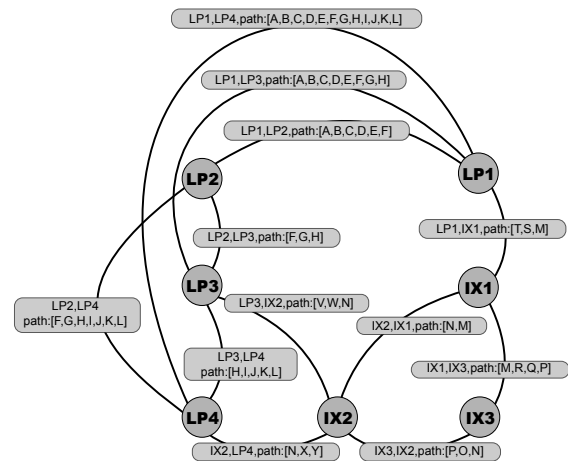


Figure 1: Graph logical representation.

by the maximum number of neighbor nodes within a geographical range.

4 GRAPH STRUCTURE AND DYNAMICS

It was assumed that Python is the nowadays language of election for fast and lightweight development. Therefore, the Internet graph was constructed using the Python package NetworkX (networkx.github.io/) which allows the creation, manipulation, and analysis of the structure and dynamics of complex networks. It was chosen a NetworkX Undirected Simple Graph for modeling the Internet nodes and inter-connections, because it is assumed that the link properties between two nodes is the same for both directions.

A NetworkX allows the addition of arbitrary attributes for graph nodes and links. Nodes will an identifier and two attributes `ntype` and `coord`, the first defines the type of node (IX or Landing Point - LP) and the second the geographic coordinate as a 2-tuple with latitude and longitude. Links (or edges under NetworkX nomenclature) are defined by the two endpoint nodes and have three attributes `etype`, `dist` and `path`, the first defines the type of the link (Ocean, Land, Land to Ocean, etc. . .), the second attribute defines the geographical distance of the link and the final attribute defines the geographical path of the link as a list of geographical coordinates. The unidirectional nature of the graph implies that the attributes between `node1` and `node2`, are the same as the ones between `node2` and `node1`. Therefore, the geographical path may have to be inverted when starting from the node considered as the end of the path.

Figure 1 depicts a logical representation of the graph, where letters represent the geographic coordinates of the respective points.

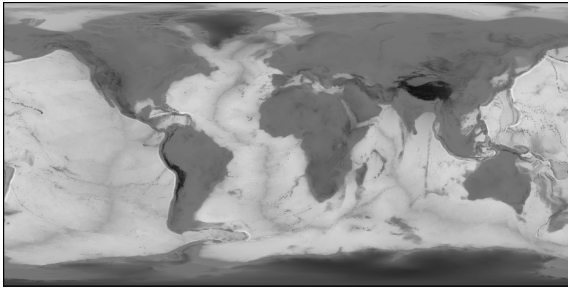


Figure 2: Earth elevation/depth map.

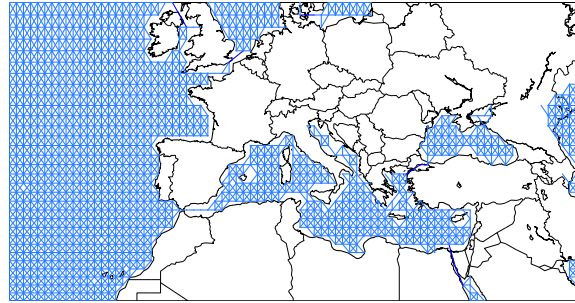


Figure 3: Ocean grid.

5 GRAPH CONSTRUCTION

Since all considered graph nodes are known they were just added to the graph with the respective attributes.

The definition of the links followed the following steps:

1. For each submarine cable determine the ocean path between all pairs of landing points. Add a graph edge for each pair with the respective ocean path attribute.
 - (a) For each landing point, determine the closest ocean grid point (ocean landing point).
 - (b) Determine its end-points. Which may be more than two.
 - (c) Determine the shortest ocean path between the endpoints that inter-connects all ocean landing points.
 - (d) Add a edge to the Internet graph for each pair of landing points using as path attribute the ocean path obtained in step 2.
2. Based on heuristic rules determine the connections between IX over land paths. Add a graph edge for each one with the respective land path attribute.
3. Based on heuristic rules determine the connections between IX and landing points over land paths. Add a graph edge for each one with the respective land path attribute.
4. Solve the cases were a node or a set of connected nodes (sub-graph) are disconnected from the main group of nodes.

Steps 1 to 4 require an underlying ocean grid and land grid to determine the paths. This grids were defined also as unidirectional NetworkX graphs to allow the estimation of the best paths in ocean or land.

Both ocean and land grids were constructed based on elevation/depth information obtained from a geographic referenced tiff from the USA National Ocean and Atmospheric Administration (NOAA) depicted

in Figure 2. All geographic distances were calculated over the Earth Rhumb line between two locations (see. Appendix).

The ocean grid construction started by defined a set of geographic underwater points from latitude -51° to 78° , and from longitude -180° to 180° in one degree intervals. An Ocean Grid edge is included if both end-points are underwater and three equally spaced points between them are also underwater. A georeferenced point is considered underwater if its (average) elevation is zero or less. This rule may erroneously include land locations that are below sea level (e.g., Netherlands), and erroneously exclude locations, subject to high tides, that are not permanently covered by water. Moreover, the choice to consider zero elevation has threshold for allow the passage of a submarine cable was a conscious one; to compensate the low resolution (high distance between grid georeferenced points) that was excluding most of the water straits and channels of the world were submarine cables pass. Even with this relax elevation rule some important water straits and channels were not considered viable to pass a submarine cable and had to be manually added. Namely:

- Add connection over the Suez channel.
- Add connection over the Panama Chanel.
- Add connection over the English Chanel.
- Add connection near Isle of Man Channel (Irish Sea to Atlantic North).
- Add connection between the sea channel between Denmark and Sweden.
- Add connection from the White Sea to Barents Sea in Russia.
- Add connection from Mediterranean Sea to Istanbul and Black Sea, over Dardanelles strait and Sea of Marmara.
- Add connection over Malacca strait between Malaysia and Indonesia Sumatra Island.
- Add connection over the strait between Indonesian islands of Sumatra and Java.

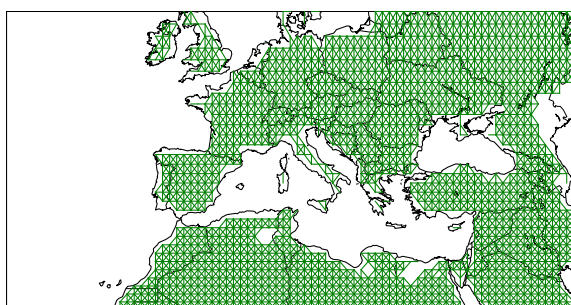


Figure 4: Land grid.

Moreover some points of Ocean Grid located in Netherlands had to be removed because they were classified as underwater, because they are below the sea level however are dry land. The resulting ocean grid had only one unconnected subgraph (isolated ocean zone), namely the Caspian Sea with 80 nodes. The final ocean grid had 31434 nodes and 119229 edges. Figure 3 depicts a zoom area of the ocean grid that includes the Atlantic ocean, seas of the north of Europe, Mediterranean sea at the south and part of the Caspian sea. Note that, in the figure is visible some of the manual edge additions, namely the Panama Channel, around great Britain islands, between Denmark and Sweden and from Mediterranean Sea to Istanbul.

The construction of the Land Grid followed a similar approach using as rule for a grid points and intermediary point an elevation higher than zero. It included geographic points above sea level points from latitude -80° to 80° , and from longitude -180° to 180° in one degree intervals. Only two major faults on the grid had to be corrected, namely the addition of long bridges (e.g., between three of Japan main islands) that transport terrestrial data cables. Namely:

- One connection between Honshu and Kyushu islands in Japan.
- One connection between Honshu and Hokkaido islands in Japan

The final land grid had 18312 nodes and 65690 edges. Figure 4 depicts a zoom area of the land grid that includes Europe and the north of Africa.

Figure 5 depicts an simple network example that will illustrate the Internet graph construction process that should lead to a resulting graph similar to the one depicted in Figure 1. The Step 1 of the Internet graph construction consists in, for all submarine cables, add a graph edge for all landing point pairs in a cable using an ocean path. In step 1a, is determined the closest point of the ocean grid to each landing point. Using Figure 5 as an example, landing points LP1, LP2, LP3 and LP4 are associated with points A, F, H, and L of the Ocean grid, respectively. In step 1b, are determined the two points with the higher distance between

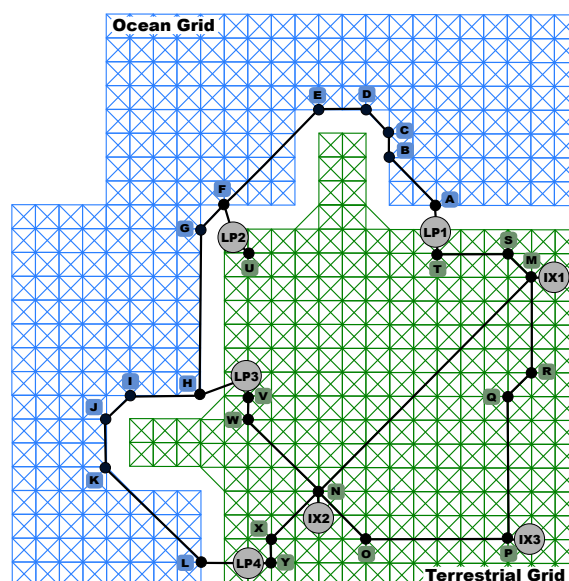


Figure 5: Ocean and terrestrial grids usage example.

them, these will be considered the main end-points of the cable (LP1 and LP4 in the example). Note that, there are submarine cables with more than two end-points. In step 1c, is determined the order and path by which the landing points are inter-connected. Starting from one of the main end-points of the cable, the algorithm searches the closest landing point, and the respective ocean points, using the ocean grid and determines the geographic path. From this new point searches for the remaining landing points the closest one, and so on until the other main end-point is reached. In the example, starting from LP1 ocean grid point A, the closest ocean point by ocean is F, therefore the next landing point of the cable with be LP2 using the Ocean path [A,B,C,D,E,F]. Then from LP2 ocean grid point F, the closest ocean point by ocean is H, therefore the next landing point of the cable with be LP3 using the Ocean path [F,G,H], and so on until LP4 is reached. However in this process, due to the existence of multiple end-points or intricate cable paths, some landing-points may be left unconnected. To discover how they inter-connect to the remaining cable landing points, a similar algorithm is used; for all pairs of connected and unconnected landing points calculate the pair with the shortest distance over ocean and connect them; repeat until all nodes are connected. In Step 1d, for all pairs of a landing points in a cable is added edge to the Internet graph using as path attribute the concatenation of geographic paths obtained from the order of interconnection and paths obtained in step 1c.

The heuristic rules for construction steps 2 and 3 used were: (i) each IX connects to a maximum of 12 IX neighbors within a 2500Km radius using land

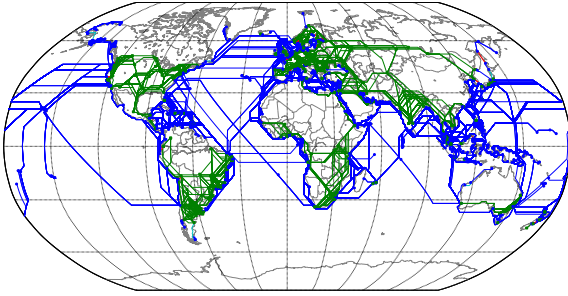


Figure 6: Final quasi-realistic Internet graph.

paths, (ii) each landing point connects to a maximum of 3 IX within a radius of 250km using a land path, and (iii) unconnected subgraphs are joined to the master graph by selecting the node closest to a main graph node within 2000Km using a land path. Large distances are required to allow the inter-connection of IX in South America and Africa where they are more further apart. The determination of the land paths between nodes starts by inferring the closest land grid point to each location, and find the shortest path using the land grid graph. In the example, IX2 connects to LP3 and LP4, from its land grid point N using paths [N,W,V] to LP3 and [N,X,Y] to LP4.

Finally in step 4, the unconnected nodes or subgraphs were merged with the main graph with a direct connection (not using the ocean or land grids) between the node closest to a main graph node and the respective closer node within 500Km. It was necessary to extend the maximum range of direct connections to 2000Km, to include a connection in Sacalina Island, Russia to inter-connect the "Far East Submarine Cable System" to the remaining nodes.

The final Internet graph constructed as 1545 nodes (600 IX, and 945 Landing Points), and 10332 edges. Figure 6 depicts the Internet graph in a world map.

6 PROOF-OF-CONCEPT RESULTS

To validate the constructed Internet graph a simple experiment was devised to see how the model allow the prediction of round trip time (RTT) and number of hops, between multiple location on Earth assuming simplistic simplifications as link and node loads uniformity and routing symmetry using the shortest path. For the measurements it were used 15 servers spread all over the world, see Figure 7. Measurements were made over a period of one week (from March 10th to March 17th 2017) using ping and traceroute, respectively.

Table 1 presents the measured (at the left) values

| City | Country | Latitude | Longitude |
|---------------|--------------|-------------|--------------|
| Amsterdam | Netherlands | 52.3702157 | 4.8951679 |
| Chicago | US | 41.8781136 | -87.6297982 |
| Frankfurt | Germany | 50.1109221 | 8.6821267 |
| Hafnarfjörður | Iceland | 64.0291054 | -21.9684626 |
| Hong-Kong | China | 22.396428 | 114.109497 |
| Johannesburg | South Africa | -26.2041028 | 28.0473051 |
| LA | US | 34.0522342 | -118.2436849 |
| London | UK | 51.5073509 | -0.1277583 |
| Madrid | Spain | 40.4167754 | -3.7037902 |
| Milan | Italy | 45.4654219 | 9.1859243 |
| Moscow | Russia | 55.755826 | 37.6173 |
| São Paulo | Brazil | -23.5505199 | -46.6333094 |
| Stockholm | Sweden | 59.3293235 | 18.0685808 |
| Tel Aviv | Israel | 32.0852999 | 34.7817676 |
| Vina del Mar | Chile | -33.0153481 | -71.5500276 |

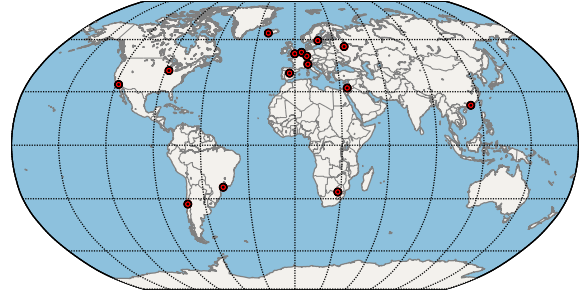


Figure 7: Test server locations.

for the average RTT in milliseconds (top) and number of nodes (bottom).

Using the Internet graph model it was estimated the path distance between all servers and the number of nodes. Assuming a speed of data propagation of 60% of the speed of light it was possible to estimate the RTT between two points. Table 1 presents the predicted (at the right) values. The average absolute error of prediction was approximately 28.8% for the RTT and 36.1% for the number of nodes. To comparison, the average absolute predicting the RTT using the direct line geographic distance between any two points (and the same speed of data propagation) were 48.3%.

7 CONCLUSIONS

This paper presented the construction process and final result of a quasi-realistic Internet graph that incorporates real infrastructure data. Such graph will allow the optimization and prediction of services that operate in a world-scale environment. A simple experiment with the graph proved that large gains in terms of prediction of Internet end-to-end metrics can be achieved. Moreover, the graph (and associated usage and construction code) is publicly available and can be expanded with additional Internet information.

As future work, the graph may be improved with localized Internet topology information made available by ISP, and with additional measurements (new or historic ones available in public repositories).

Table 1: Measured (left) and predicted (right) values for the average RTT in milliseconds (top) and number of nodes (bottom) between multiple locations.

| | Amsterdam | Chicago | Chile | Frankfurt | Hong-Kong | Iceland | Israel | Johannesburg | LA | London | Madrid | Milan | Moscow | São Paulo | Sweden |
|--------------|----------------------|----------------------|----------------------|----------------------|----------------------|----------------------|----------------------|----------------------|----------------------|----------------------|----------------------|----------------------|----------------------|----------------------|----------------------|
| Amsterdam | - | 103.0/130.0 13/13 | 204.9/208.8 18/15 | 18.0/9.9 5/5 | 309.1/177.7 12/19 | 36.1/39.6 6/6 | 65.2/87.8 8/15 | 172.7/208.6 8/18 | 153.4/174.7 12/18 | 6.5/7.4 13/5 | 31.5/29.7 7/7 | 24.1/21.6 7/8 | 46.3/49.6 5/12 | 231.8/171.4 12/12 | 22.8/36.9 6/10 |
| Chicago | 103.1/130.0 12/13 | - | 139.7/157.6 19/12 | 109.1/133.2 14/14 | 206.1/300.9 19/28 | 124.9/166.0 13/16 | 159.2/211.0 16/24 | 261.2/289.7 16/17 | 66.8/46.0 15/6 | 96.3/123.1 17/9 | 110.7/133.5 14/10 | 112.3/136.9 16/13 | 149.9/172.9 17/21 | 144.9/167.9 13/13 | 118.1/152.6 13/14 |
| Chile | 467.7/208.8 16/15 | 142.5/157.6 19/12 | - | 216.2/207.9 22/14 | 472.3/371.1 17/27 | 588.7/244.2 13/17 | 216.3/281.2 17/23 | 763.5/206.1 19/11 | 178.0/157.4 18/11 | 700.2/206.4 16/15 | 225.1/182.6 21/10 | 220.8/203.2 13/12 | 392.2/245.0 14/21 | 255.2/43.5 16/5 | 272.3/236.0 15/20 |
| Frankfurt | 6.9/9.9 7/5 | 109.8/133.2 14/14 | 214.5/207.9 20/14 | - | 311.2/168.3 22/15 | 48.3/43.1 9/6 | 66.1/78.4 10/11 | 200.6/199.2 12/14 | 157.0/177.9 17/19 | 15.5/10.7 15/6 | 29.7/29.0 9/6 | 16.3/12.3 11/4 | 42.4/40.2 4/8 | 237.5/170.5 15/11 | 20.7/44.0 5/11 |
| Hong-Kong | 307.0/177.7 12/19 | 189.0/300.9 14/28 | 327.5/371.1 23/27 | 304.1/168.3 24/15 | - | 314.6/210.8 13/20 | 349.7/131.4 17/8 | 434.3/230.3 15/11 | 160.9/217.3 13/4 | 271.6/178.4 15/20 | 267.7/192.1 24/19 | 283.1/172.7 13/16 | 316.0/141.3 14/9 | 324.5/333.7 16/24 | 309.9/159.9 15/14 |
| Iceland | 35.9/39.6 6/6 | 124.7/166.0 14/16 | 244.8/244.2 19/17 | 47.7/43.1 11/6 | 299.0/210.8 15/20 | - | 112.7/120.9 13/16 | 238.5/241.7 12/19 | 178.7/210.8 17/21 | 40.1/43.5 13/8 | 64.2/65.2 11/9 | 50.5/54.8 9/9 | 86.4/82.8 9/13 | 230.0/206.8 13/14 | 64.0/73.0 13/13 |
| Israel | 65.3/87.8 7/15 | 159.6/211.0 18/24 | 407.1/281.2 19/23 | 64.7/78.4 8/11 | 343.4/131.4 17/8 | 109.0/120.9 10/16 | - | 241.1/113.7 11/8 | 211.0/255.8 11/29 | 64.6/88.5 13/16 | 105.1/102.2 10/15 | 76.1/82.8 12/12 | 115.2/52.1 7/6 | 267.4/243.8 14/20 | 87.1/70.2 9/10 |
| Johannesburg | 183.2/208.6 7/18 | 260.1/289.7 15/17 | 388.9/206.1 20/11 | 246.0/199.2 12/14 | 444.9/230.3 14/11 | 239.1/241.7 10/19 | 244.2/113.7 11/8 | - | 337.6/320.1 18/18 | 176.1/209.3 11/19 | 202.8/159.8 9/9 | 204.6/203.6 10/15 | 237.9/172.9 8/9 | 367.1/168.7 12/8 | 205.3/190.7 14/13 |
| LA | 156.9/174.7 11/18 | 70.7/46.0 14/6 | 174.7/157.4 21/11 | 152.4/177.9 20/19 | 151.4/217.3 12/21 | 177.2/210.8 12/21 | 217.5/255.8 15/29 | 351.9/320.1 18/18 | - | 195.4/167.9 18/14 | 178.6/178.2 23/15 | 176.4/181.7 10/18 | 193.7/217.6 11/26 | 177.3/167.7 15/12 | 185.9/197.4 13/19 |
| London | 6.4/7.4 11/5 | 87.8/123.1 17/9 | 235.8/206.4 26/15 | 15.2/10.7 10/6 | 259.2/178.4 15/20 | 40.1/43.5 13/8 | 70.1/88.5 14/16 | 176.4/209.3 12/19 | 158.2/167.9 19/14 | - | 35.1/27.4 14/7 | 21.8/22.4 13/9 | 44.6/50.4 12/13 | 184.4/169.1 17/14 | 28.6/30.1 12/6 |
| Madrid | 31.5/29.7 9/7 | 110.8/133.5 15/10 | 224.8/182.6 20/10 | 27.2/29.0 10/6 | 271.3/192.1 10/19 | 64.2/65.2 11/9 | 107.7/102.2 11/15 | 203.0/159.8 13/9 | 172.6/178.2 18/15 | 35.2/27.4 10/7 | - | 24.4/23.5 11/4 | 72.9/66.1 13/13 | 223.6/145.2 16/7 | 53.5/56.9 8/12 |
| Milan | 19.7/21.6 13/8 | 112.2/136.9 18/13 | 223.0/203.2 23/12 | 16.5/12.3 13/4 | 288.1/172.7 16/16 | 50.5/54.8 9/9 | 68.6/82.8 13/12 | 204.3/203.6 11/15 | 168.0/181.7 17/18 | 22.9/22.4 12/9 | 24.4/23.5 8/4 | - | 51.4/46.6 10/10 | 233.9/165.8 13/9 | 36.5/50.5 12/13 |
| Moscow | 52.2/49.6 5/12 | 149.2/172.9 18/21 | 270.0/245.0 23/21 | 42.0/40.2 7/8 | 325.2/141.3 17/9 | 83.6/82.8 10/13 | 122.4/52.1 8/6 | 235.1/172.9 10/9 | 197.3/217.6 18/26 | 44.5/50.4 13/13 | 72.7/66.1 9/13 | 57.8/46.6 10/10 | - | 267.4/207.6 14/18 | 65.6/25.8 6/6 |
| São Paulo | 233.5/171.4 11/12 | 144.6/167.9 18/13 | 406.5/433.5 16/5 | 241.3/170.5 21/11 | 330.4/333.7 20/24 | 236.5/206.8 12/14 | 273.4/243.8 16/20 | 370.8/168.7 14/8 | 174.5/167.7 19/12 | 184.1/169.1 18/12 | 224.0/145.2 21/7 | 221.6/165.8 12/9 | 262.9/207.6 13/18 | - | 228.4/198.6 18/17 |
| Sweden | 22.8/36.9 6/10 | 113.9/152.6 13/14 | 232.2/236.0 24/20 | 20.6/44.0 6/11 | 314.8/159.9 17/14 | 64.2/73.0 11/13 | 89.0/70.2 9/10 | 205.1/190.7 13/13 | 177.5/197.4 16/19 | 28.1/30.1 12/6 | 53.4/56.9 7/12 | 39.5/50.5 11/13 | 75.7/25.8 6/6 | 225.5/198.6 14/17 | - |

ACKNOWLEDGEMENTS

This work was supported by the Fundação para Ciência e Tecnologia (FCT) through PTDC/EEI-TEL/5708/2014 and UID/EEA/50008/2013.

REFERENCES

- Durairajan, R., Barford, P., Sommers, J., and Willinger, W. (2015). Intertubes: A study of the us long-haul fiberoptic infrastructure. *SIGCOMM Comput. Commun. Rev.*, 45(4):565–578.
- Durairajan, R., Ghosh, S., Tang, X., Barford, P., and Eriksson, B. (2013). Internet atlas: A geographic database of the internet. In *Proceedings of the 5th ACM Workshop on HotPlanet, HotPlanet '13*, pages 15–20, New York, NY, USA. ACM.
- Pilosov, A. and Kapela, T. (2008). Stealing The Internet - An Internet-Scale Man In The Middle Attack. In *DEFCON16*.
- Salvador, P. and Nogueira, A. (2014). Customer-side detection of internet-scale traffic redirection. In *16th International Telecommunications Network Strategy and Planning Symposium (NETWORKS 2014)*.

APPENDIX

Geographic Distance over Earth Rhumb Line

Considering two geographic points with latitude ψ_1^o and longitude λ_1^o (in degrees), and latitude ψ_2^o and longitude λ_2^o (in degrees). The geographic coordinates for both points in radians are given by:

$$(\psi_1, \lambda_1) = (\psi_1^o \pi / 180, \lambda_1^o \pi / 180)$$

$$(\psi_2, \lambda_2) = (\psi_2^o \pi / 180, \lambda_2^o \pi / 180)$$

The longitude difference using the shortest route (East to West, or West to East) is given by:

$$\Delta\lambda = \min(\text{mod}(\lambda_2 - \lambda_1, 2\pi), \text{mod}(\lambda_1 - \lambda_2, 2\pi))$$

And the latitude difference is given by:

$$\Delta\psi = \psi_2 - \psi_1$$

The projected latitude difference is given by:

$$\Delta\phi = \ln \left(\frac{\tan(\psi_1/2 + \pi/4)}{\tan(\psi_2/2 + \pi/4)} \right)$$

The geographic distance over a Rhumb line is then given by:

$$d = \begin{cases} R \sqrt{\cos(\psi_1)^2 \Delta\lambda^2 + \Delta\psi^2}, & \text{if } \Delta\phi < \rho \\ R \sqrt{\left(\frac{\Delta\psi}{\Delta\phi}\right)^2 \Delta\lambda^2 + \Delta\psi^2}, & \text{otherwise} \end{cases}$$

where R is the mean radius of Earth (6371 Km) and ρ must be the smallest number resolution (e.g., 10^{-20}). A close to zero projected latitude difference ($\Delta\phi < \rho$) means that the path between the points is parallel to the equator line.